Journal of Medicinal Chemistry

Article

pubs.acs.org/jmc

Cyclic Peptides Incorporating Phosphotyrosine Mimetics as Potent and Specific Inhibitors of the Grb7 Breast Cancer Target

Gabrielle M. Watson,[†] Menachem J. Gunzburg,[†] Nigus D. Ambaye,[†] William A. H. Lucas,[†] Daouda A. Traore,[†] Ketav Kulkarni,[†,‡] Katie M. Cergol,[§] Richard J. Payne,[§] Santosh Panjikar,[†,∥] Stephanie C. Pero,[⊥] Patrick Perlmutter,[‡] Matthew C. J. Wilce,[†] and Jacqueline A. Wilce*[,†]

[†]Department of Biochemistry and Molecular Biology and [‡]School of Chemistry, Monash University, Melbourne, Victoria 3800, Australia

[§]School of Chemistry, The University of Sydney, Sydney, New South Wales 2006, Australia

[∥]Australian Synchrotron, 800 Blackburn Road, Clayton, Victoria 3168, Australia

[⊥]Department of Surgery and Vermont Cancer Center, University of Vermont, Burlington, Vermont 05401, United States

Supporting Information

ABSTRACT: The Grb7 adaptor protein is a therapeutic target for both TNBC and HER2+ breast cancer. A nonphosphorylated cyclic peptide **1** (known as G7−18NATE) inhibits Grb7 via targeting the Grb7-SH2 domain, but requires the presence of phosphate ions for both affinity and specificity. Here we report the discovery of malonate bound in the phosphotyrosine binding pocket of the apo-Grb7-SH2 structure. Based on this, we carried out the rational design and synthesis of two analogues of peptide **1** that incorporate carboxymethylphenylalanine (cmF) and carboxyphenylalanine (cF) as mimics of phosphotyrosine (pY). Binding studies using SPR confirmed that affinity for Grb7-SH2 domain is improved up to 9-fold over peptide **1** under physiological phosphate conditions (K_D = 2.1−5.7 μM) and that binding is specific for Grb7-SH2 over closely related domains (low or no detectable binding to Grb2-SH2 and Grb10-SH2). X-ray crystallographic structural analysis of the analogue bearing a cmF moiety in complex with Grb7-SH2 has identified the precise contacts conferred by the pY mimic that underpin this improved molecular interaction. Together this study identifies and characterizes the tightest specific inhibitor of Grb7 to date, representing a significant development toward a new Grb7-targeted therapeutic.

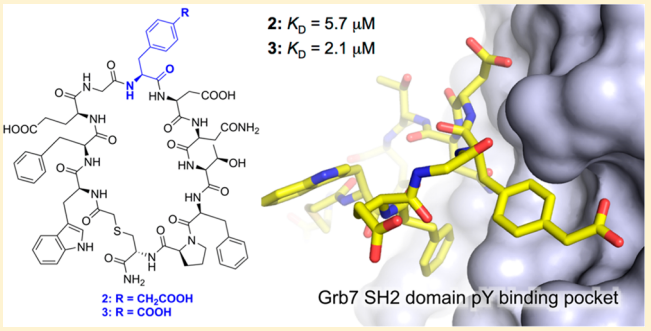

INTRODUCTION

Tumor development and progression into a metastatic and malignant state involves deregulation of signaling pathways governing cell proliferation, migration, and survival.[1] Key signaling proteins that are aberrantly overexpressed or act at critical junctions in cancer are therefore of interest for their potential as therapeutic targets. The multiadaptor protein Grb7 (growth factor receptor bound protein 7) operates via distinct signaling pathways to induce cell proliferation and migration in the progression of a variety of cancer types including the breast cancer subclasses HER2+ and triple negative breast cancer (TNBC).[2,3] In HER2+ cell lines, Grb7 is co-overexpressed with HER2, the well-known predictor for a poor prognosis in breast cancer patients, with Grb7 facilitating aberrant proliferative signaling.[4,5] The removal or inhibition of Grb7 has been shown to reduce breast cancer cell viability and increase the activity of anti-HER2 cancer therapeutics.[6,7] Grb7 has also been shown to play an important role in the migratory potential of cancer cells.[8] In both HER2+ and TNBC cell lines, inhibition of Grb7 impairs cell migration and invasion as well as colony growth.[3,9] Furthermore, in a mouse model of pancreatic cancer, Grb7 inhibition reduced cancer cell metastasis.[10] Clinical investigations have shown that Grb7 overexpression is significantly associated with a higher clinical stage and larger tumor size for patients with breast cancer, and is a significant predictor for reduced cancer-free periods.[11] Thus, Grb7, which acts at the nexus of both growth and migratory signaling pathways, has been identified as a therapeutic target for the treatment of several cancer types including both HER2+ and TNBC.[3,12]

Grb7 is a 532 amino acid multidomain protein possessing an N-terminal proline-rich domain, a Ras-associating-like (RA) domain, a pleckstrin homology (PH) domain, and a C-terminal src-homology 2 (SH2) domain. It is through the C-terminal SH2 domain that Grb7 interacts with its upstream receptor tyrosine kinases and other signaling molecules including HER2, HER3, EGFR, and FAK, allowing Grb7 to propagate downstream signaling.[8,13−15] It is the SH2 domain, therefore,

Received: April 20, 2015

DOI: 10.1021/acs.jmedchem.5b00609
J. Med. Chem. XXXX, XXX, XXX−XXX

Table 1. Summary of Crystallographic Information

data collection	Apo Grb7-SH2	Grb7-SH2: **2**
wavelength	0.954	0.954
space group	$P6_3$	$P2_12_12_1$
unit cell dimensions		
a, *b*, *c* (Å)	83.99 83.99, 75.95	55.48, 68.89, 77.04
α, β, γ (deg)	90, 90, 120	90, 90, 90
Resolution (Å)	28.17−1.80 (1.9−1.8)	43.21−2.55 (2.641−2.55)
R_{merge}[a] (%)	10.6 (54.9)	11.07 (65.92)
I/σI	16.7 (4.9)	11.71 (3.23)
unique reflections measured	28306 (4125)	10038 (996)
completeness (%)	100 (100)	99.53 (99.80)
multiplicity	11.3 (11.3)	8.9 (9.3)
Refinement		
R_{work} (%)	17.60 (20.49)	21.17 (28.31)
R_{free} (%)	20.63 (22.52)	25.81 (34.72)
No. of atoms		
protein	1809	1810
ligand (MLA)	7	50
solvent	130	29
Mean B-factors (Å^2)		
protein	20.70	45.80
ligand (MLA)	15.90	52.80
solvent	26.60	38.70
RMSDs		
bond lengths (Å)	0.007	0.010
bond angles (deg)	1.27	1.27
Ramachandran plot (%)		
favored regions	98.7	98.0
allowed regions	0.9	0

[a] $R_{merge} = \Sigma_{hkl} \Sigma_i |I_i(hkl) - \langle I(hkl)\rangle| / \Sigma_{hkl} \Sigma_i I_i(hkl)$. where $I_i(hkl)$ is the *i*th intensity measurement of reflection *hkl*, $\langle I(hkl)\rangle$ its average. Values given in brackets are for the high resolution shell.

that has been the target for inhibitor development to date.[16,17] SH2 domains are ∼100 amino acid domains that recognize phosphotyrosine (pY) residues of upstream binding partners with surrounding amino acid residues contributing to substrate specificity.[18] In the case of the Grb7-SH2 domain (residues 416−532), sequences with a pYXN motif that occur in a turn conformation are preferentially targeted.[19] This feature guided the development of a nonphosphorylated cyclic peptide **1** (termed G7−18NATE), that targets the SH2 domain of Grb7 over closely related Grb2- and Grb14-SH2 domains.[20] The 11-residue peptide (WFEGYDNTFPC), cyclized via a thioether bond from the N-terminus to the C-terminal thiol side chain of cysteine, binds the Grb7-SH2 domain with micromolar affinity, with a reported equilibrium dissociation constant (K_D) of 347−4.1 μM depending upon the buffer conditions utilized.[21−23] Promisingly, in cellular assays, peptide **1** conjugated to the cell permeability sequence Penetratin, reduced cell migration in both HER2+ and TNBC cell lines, and showed co-operative effects with the anticancer therapeutics doxorubicin and Herceptin in HER2+ cell lines.[2,3,7] The cell permeable peptide **1** has also been tested in a mouse model of pancreatic cancer, resulting in reduction in the number and size of pancreatic tumors.[10] Hence, peptide **1** is a successful peptide for inhibiting Grb7 in breast cancer assays, and a promising starting point for therapeutics targeting TNBC and HER2+ breast cancer.

Upon further investigation of the dependence of the peptide **1** interaction with Grb7-SH2 on the buffer conditions used, the low micromolar binding (K_D = 4 μM) and specificity of peptide **1** for Grb7 was discovered to only occur in the presence of high concentrations of phosphate (50 mM).[24] In the absence of phosphate, the affinity of peptide **1** for the Grb7-SH2 domain was reduced to K_D > 200 μM and selectivity for Grb7-SH2 over Grb2-, Grb10-, and Grb14-SH2 was lost. It was speculated that the phosphate from the buffer was acting at the pY binding pocket of the Grb7-SH2 domain, to stabilize the BC loop at the peptide binding site (note that the nomenclature used is as derived by Eck et al. for SH2 domain secondary structure).[25] Indeed, a previously reported structure of the apo-Grb7-SH2 domain revealed a sulfate ion bound at this site that appeared to constrain the BC loop in an optimal conformation for peptide binding.[21] Thus, in order to improve the potential of peptide **1** for therapeutic use, we predicted that the addition of a negatively charged or electronegative group appended to the inhibitor peptide tyrosine would improve peptide **1** binding selectivity and affinity under physiological phosphate conditions. Such phosphotyrosine (pY) mimetics have been used in the development of other SH2 domain inhibitors and are favored over pY itself, since the phosphate group would likely render the inhibitor peptide impermeable to cellular membranes and unstable due to constitutive phosphatase activity inside cells and therefore not efficacious in cellular or animal studies.[26]

Here we report the design, synthesis, and characterization of two peptide **1** analogues that incorporate carboxylic acid-based phosphotyrosine (pY) mimetics (carboxymethylphenylalanine (cmF) and carboxyphenylalanine (cF)) and show improved binding of these analogues to Grb7-SH2 under physiological conditions. Our choice of pY mimetic was guided by the high-

DOI: 10.1021/acs.jmedchem.5b00609
J. Med. Chem. XXXX, XXX, XXX−XXX

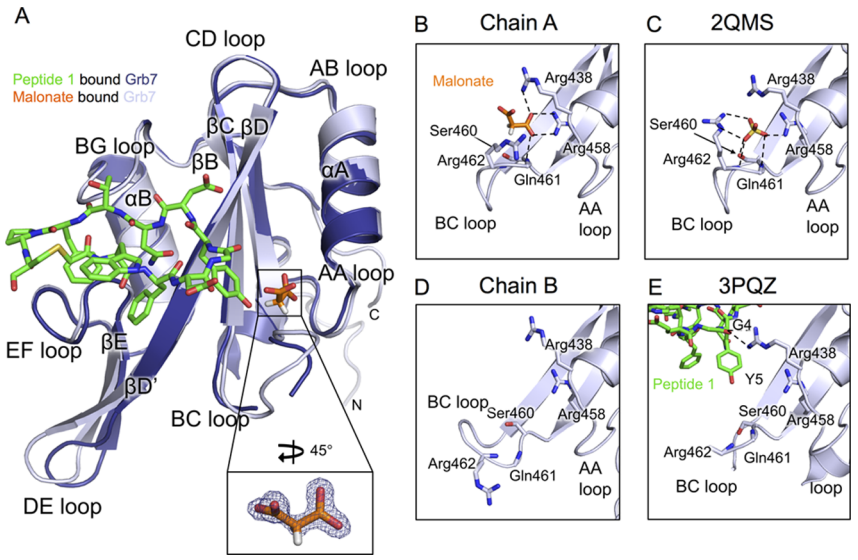

Figure 1. Structure based rationale for a functionalized peptide 2 derivative. (A) Structural overlay of the 2.4 Å Grb7-SH2:peptide **1** domain complex (PDB ID 2QMS: green sticks and purple cartoon, respectively) and the 1.8 Å apo-Grb7-SH2 structure (PDB ID 4WWQ: blue-white cartoon) with malonic acid (orange sticks) in the pY binding pocket. The inset shows the 2Fo-Fc map surrounding malonic acid contoured at 2σ; (B−E) Detail of the pY binding pocket: (B) Malonic acid bound Grb7-SH2, Chain A PDB ID: 4WWQ; (C) Sulfate bound Grb7-SH2, PDB: 2QMS; (D) Ligand free Grb7-SH2, Chain B PDB: 4WWQ; (E) peptide **1** bound Grb7-SH2, PDB: 3PQZ. Key amino acids are shown as sticks and hydrogen bonds as dashed lines.

resolution X-ray crystal structure of the Grb7-SH2 domain that was crystallized in the presence of the dicarboxylic acid, malonate. The malonate ion was discovered to reside precisely in the Grb7-SH2 pY binding pocket making similar contacts to surrounding residues as a sulfate or phosphate ion would. This inspired the design and synthesis of cmF peptide analogue **2** and cF peptide analogue **3**. The pY mimicking residues within the cyclic peptides would be expected to provide a negative charge for forming interactions in the pY binding pocket at physiological pH, but would neither interfere with the ability of the peptide to cross cell membranes nor compromise in vivo stability of the analogue.

We demonstrate that peptides **2** and **3** indeed bind with enhanced affinity to the Grb7-SH2 domain compared with peptide **1** under physiological phosphate concentrations, and that increased phosphate levels compete with the peptides for Grb7-SH2 domain binding. We also demonstrate that they retain their preferential binding to the Grb7-SH2 domain compared to the SH2 domains of the closely related Grb2 and Grb10. We furthermore report the X-ray crystal structure of cmF bearing analogue **2** in complex with the Grb7-SH2 domain. This demonstrates the binding mode of peptide **2** with the target and, in particular, the way in which the cmF group extends into the phosphotyrosine binding cleft forming additional contacts with core binding pocket residues. The cmF and cF containing peptides **2** and **3** thus represent the highest affinity inhibitors of Grb7 to date that possess specificity for Grb7 under physiological conditions. Cell permeable forms of these peptides will provide both a powerful tool for studies of Grb7 inhibition in cells and underpin future steps toward the development of a new therapeutic targeted to Grb7 for the treatment of HER2+ and TNBC.

RESULTS

Apo-Grb7-SH2 Domain Crystal Structures Reveals Both a Bound Malonate as well as a Truly "apo" SH2 Domain. In the course of our investigation of the Grb7-SH2 domain, we grew high quality crystals of the apoprotein for structure determination using crystallization conditions that included the dicarboxylic acid malonate. The protein crystallization and data collection statistics have been reported previously.[27] The apo-Grb7-SH2 domain crystal structure was solved to 1.8 Å using molecular replacement with PDB ID 2QMS as the search model. The refinement statistics are provided in Table 1 and the coordinates are deposited in the Protein database (PDB ID: 4WWQ). Interestingly, the asymmetric unit contains two chains of Grb7-SH2 (residues 421−532 in chain A and 415−532 in chain B visible in the electron density): chain A which contains malonate in the phosphotyrosine binding site, and chain B that contains no ligand and is thus a truly "apo" structure.

The chains both adopt the typical SH2 domain fold, with $\alpha\beta\beta\beta\beta\alpha$ topology (Figure 1A). Each chain is part of a noncovalent dimer with a chain from an adjacent asymmetric unit (chain A from one asymmetric unit to chain B of another). The noncovalent dimer forms through an interface centered on F511 (αB8) as has also been observed in all other crystal structures of Grb7 family member SH2 domains and has also been shown to form in solution.[28−30] Interestingly, chains A and B within the asymmetric unit are also covalently linked through a disulfide bond that occurs between C526 in chain A and C527 in chain B. This occurrence is assumed to be a crystallization artifact and not physiologically relevant, since the cellular environment is reducing, but it may have played a role in stabilizing the crystal and contributed to the quality of the diffraction. It has not been seen previously in crystal forms of the Grb7-SH2 domain.

The presence of malonate is an outcome of the crystallization condition that contained tacsimate, and it is unsurprising to observe this anion accommodated in the positively charged pY binding pocket. More surprising is the absence of this ligand in the second chain; however, the occurrence of ligand-bound alongside ligand-free protein chains in crystal structures is the result of the protein packing arrangement in which the ligand at

DOI: 10.1021/acs.jmedchem.5b00609
J. Med. Chem. XXXX, XXX, XXX−XXX

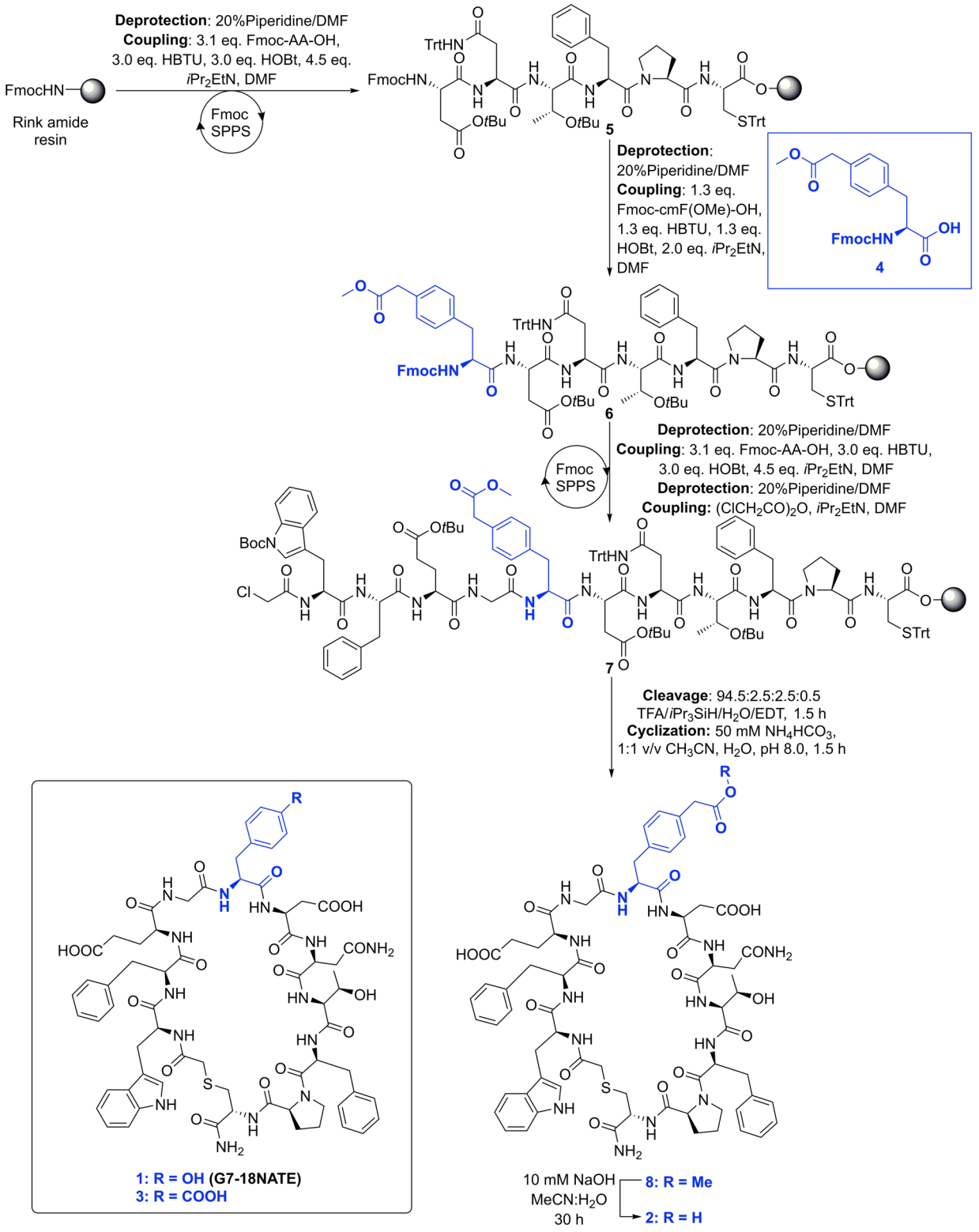

Figure 2. Chemical structures and synthesis of peptide **2**. Shown is the synthetic pathway used for the preparation of the cmF containing peptide **2**. The suitably protected carboxymethylphenylalanine building block (**4**), for incorporation into the peptide target, is highlighted in blue. Also shown, in the inset, are the chemical structures of peptide **1** and the cF containing peptide **3**.

one binding site partially occludes the binding site of the adjacent molecule, an occurrence that has been observed previously.[31] Thus, as well as providing a higher resolution structure for apo-Grb7-SH2 than previously achieved (PDB ID: 2QMS; 2.1 Å resolution) this structure reveals the way in which a carboxylic acid group can be bound in the pY binding pocket of the Grb7-SH2 domain.

Malonate Mimics Phosphate in the pY Binding Pocket of the Grb7-SH2 Domain. In chain A of the apo-Grb7-SH2 model, clear electron density allows malonate to be placed

DOI: 10.1021/acs.jmedchem.5b00609
J. Med. Chem. XXXX, XXX, XXX−XXX

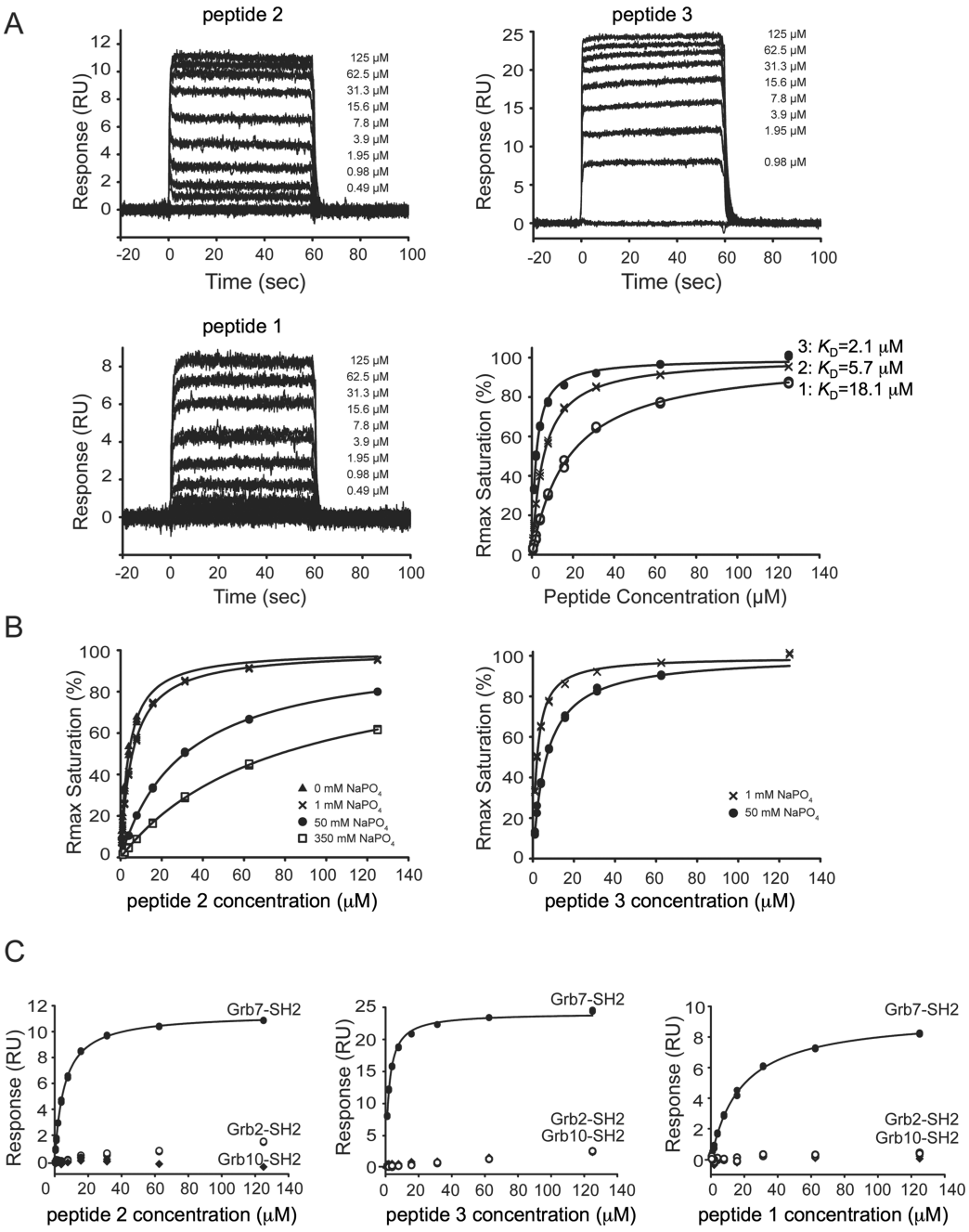

Figure 3. SPR binding analysis of peptides **1**, **2**, and **3** binding to Grb7-, Grb2-, and Grb10-SH2 domains. (A) Sensorgrams of peptide **1** (bottom left), peptide **2** (top left), and peptide **3** (top right) at varying concentrations binding the Grb7-SH2 domain at 1 mM phosphate concentration, and the corresponding equilibrium binding curves (bottom right). (B) Equilibrium binding curves for peptide **2** (left) and peptide **3** (right) binding the Grb7-SH2 domain under buffers containing different concentrations of phosphate. All buffers contained 150 mM NaCl and 1 mM DTT. (C) Equilibrium binding curves for peptide **1** (right), peptide **2** (left), and peptide **3** (center) binding the SH2 domains of Grb7, Grb2, and Grb10 under 1 mM phosphate concentration. Sensorgrams for all experiments are supplied as Supporting Information.

unambiguously in the pY binding pocket (Figure 1A - inset). The malonate forms ionic interactions and hydrogen bonds with Arg458 (βB5) and Arg438 (αA2) guanidino side chains and the backbone NH of Gln461 (BC1) (Figure 1B). This appears to hold the BC loop (residues 460−466) in a rigid position, similarly to the Grb7-SH2 domain solved with a sulfate ion bound in the pY binding pocket (PDB ID: 2QMS; the BC loop of the apo-Grb7 SH2 chain A and the BC loop of the 2QMS chain A have a Cα atom RMSD of 0.358 Å.) (Figure 1C).[21] In the 2QMS structure the sulfate was engaged in salt bridge interactions with the guanadino side chains of Arg458 (βB5) and Arg462 (BC2), and H-bonding interactions with the Gln461 backbone NH (BC1) and also the Ser460 side chain hydroxyl (βB7). The fact that Arg462 (BC2) is observed to engage the sulfate, but not the malonate ion, is likely an artifact of the malonate-containing crystal form with Arg438 (αA2) of a symmetry-related chain B forming salt bridge interactions with the second carboxylic acid of the malonate instead of Arg462 (BC2). Overall, although there are some differences in the amino acids involved in the interactions, both of these anionic ligands are able to hold the BC loop in a position that is understood to represent the ligand binding conformation.[32]

DOI: 10.1021/acs.jmedchem.5b00609
J. Med. Chem. XXXX, XXX, XXX−XXX

pY Binding Site of the apo-Grb7-SH2 Domain Adopts an "Open" Conformation. In chain B of the apo-Grb7-SH2 domain structure the BC loop adopts an alternative conformation (Figure 1D). With an empty pY binding pocket, the side chains of Arg458 (βB5), Arg462 (BC2), and Ser460 (βB7) are all directed into the solvent, and Arg438 (αA2) forms salt bridge interactions with the symmetry related chain A (explaining why the ligand binding site of chain B is empty). As a consequence, the BC loop adopts a more open structure with a Cα RMSD of 2.503 Å between the chain B BC loop (residues 460−466) compared with the chain A BC loop. This is similar to the peptide **1** bound form of Grb7-SH2 that contains no anion in the pY site (PDB ID: 3PQZ; 2.4 Å resolution), in which these pY binding pocket amino acid residues are not engaged in hydrogen bonding except for Arg438 (αA2) that forms a bond with the backbone carbonyl of G4 of peptide **1**. (Note that in discussing protein−ligand interactions, the protein will be referred to in three-letter code and the peptide ligand in one-letter code to distinguish them). In this structure the BC loop is also in an "open" configuration and displays some disorder with Asn463 (BC3) not visible in the electron density (Figure 1E).

cmF and cF residues Are Predicted as pY Mimetics for Grb7-SH2 Inhibition. Thus, the current Grb7-SH2 domain structure reveals that an anionic ligand can form several interactions in the pY binding site. We therefore predicted that either a cmF or cF residue could serve to enhance the binding of peptide **1** to the Grb7-SH2 domain and this designed peptides **2** and **3** (Figure 2). CmF has been previously observed to enhance SH2 domain-binding affinity in the case of a Grb2-targeted peptide and cF has also been used to enhance binding to an SH2 domain at the Y+3 position.[33,34] From our structural analysis of the separately determined position of peptide **1** Y5 and malonate in the pY binding site of the Grb7-SH2 domain we can see that malonate is positioned 2.5 Å beyond the Y5 hydroxyl oxygen at an approximate angle of 130° (as depicted in the superposed structures shown in Figure 1A). Thus, a cmF could mimic (or a cF closely mimic) this spatial relationship and potentially enhance the binding of peptide **1**.

Synthesis of Target Cyclic Peptides 2 and 3. Based upon this structural information a suitably protected cmF building block, Fmoc-cmF(OMe)-OH **4**, was synthesized that could be directly incorporated into Fmoc-solid-phase peptide synthesis to serve as a pY mimetic. Specifically, the building block was incorporated into peptide **1** at the Y5 position resulting in target cyclic peptide **2**. In this target the thioether linkage and remaining 10 amino acids were unchanged to allow for direct comparison with peptide **1**. Synthesis of the target amino acid Fmoc-cmF(OMe)-OH **4**, whereby the side chain carboxylic acid was protected as the corresponding methyl ester, was carried out from Boc-Tyr-O*t*Bu using slight modifications to a method previously reported by Tilley and co-workers.[35] Target cyclic peptide **2** was then prepared using Fmoc-SPPS on a Rink amide resin and subject to N-terminal chloroacetylation after the removal of the N-terminal Fmoc group (Figure 2). Resin bound hexapeptide **5** was first assembled using an excess of the commercially available protected amino acids with HBTU and HOBt as the coupling reagents and 20% piperidine in DMF for Fmoc-deprotection. Fmoc-cmF(OMe)-OH **4** was next coupled using only a slight excess of the building block and coupling reagents to afford resin bound **6**. From here, elongation of the desired peptide sequence and N-terminal chloroacetylation provided the resin bound peptide **7**. After cleavage from the resin, thioether cyclization between the N-terminal chloroacetyl moiety and the C-terminal thiol was achieved in aqueous basic conditions to produce peptide **8** and the methyl ester side chain of the cmF residue was gently saponified using dilute aqueous sodium hydroxide. The target cyclic peptide **2** was purified by reverse-phase HPLC and produced in a 7% yield based on the original resin loading. The peptide was shown to possess suitable purity (>95%) by LC-MS analysis.

Cyclic peptide **3**, bearing a cF residue in place of the cmF present in **2**, was produced using solid-phase peptide synthesis by Wuxi Nordisk Biotech to >95% purity based on LC-MS analysis.

Target Cyclic Peptides 2 and 3 Show Enhanced Binding to the Grb7-SH2 Domain under Physiological Phosphate Conditions. Surface plasmon resonance (SPR) was utilized to measure differences in affinity for the Grb7-SH2 domain between peptide **1** and the target cyclic peptides **2** and **3**. GST-fused Grb7-SH2 domain was captured on the chip surface using anti-GST antibodies, as previously established for measuring Grb7-SH2:peptide interactions.[22] Figure 3A shows that peptides **1**, **2**, and **3** each rapidly reach GST-Grb7-SH2 binding equilibrium upon peptide injection. This allows the response at equilibrium to be determined and binding curves constructed for K_D determination by fitting a single-site binding model (Figure 3A - bottom right).

In a buffer containing 1 mM phosphate at pH 7.4, peptide **2** bound to Grb7-SH2 with an affinity of K_D = 5.7 μM and peptide **3** bound to Grb7-SH2 with an affinity of K_D = 2.1 μM. Under the same conditions peptide **1** bound at a K_D = 18.1 μM (Table 2). The substitution of cmF and cF for Y thus confer a 3-fold and 9-fold enhancement of binding over peptide **1**, respectively, under physiologically relevant phosphate conditions.

Table 2. SPR Binding Studies to Investigate the Cyclic Peptides 2 and 3: Grb7-SH2 Interaction

	affinity dissociation constant[b] (μM)		
buffer[a]	1	2	3
20 mM Tris	347[c]	3.9 ± 0.05	Not measured
50 mM $NaPO_4$	2.9 ± 0.004	31.1 ± 0.07	6.57 ± 0.02
350 mM $NaPO_4$	2.6 ± 0.01	77.3 ± 0.8	Not measured
20 mM Tris, 1 mM $NaPO_4$	18.1 ± 0.1	5.7 ± 0.03	2.1 ± 0.006

[a]All buffers contained 150 mM NaCl and 1 mM DTT. [b]K_D was derived from fits to single-site saturation model. Errors are standard errors arising from the fits. [c]Reported by Gunzburg et al. (2012) under the same experimental conditions.

Phosphate is Not Required for the Binding of Cyclic Peptides 2 and 3 to the Grb7-SH2 Domain. We have previously determined that peptide **1** binding to the Grb7-SH2 domain is enhanced by the presence of phosphate in the buffer.[24] This can be rationalized by the presence of a phosphate ion in the pY binding site that enhances peptide binding by stabilizing the BC loop. In the case of peptide **1**, binding to Grb7-SH2 was previously reported to range from K_D = 4.1 μM in 100 mM phosphate to 347 μM in the absence of any phosphate.[24] In the case of peptides **2** and **3** it was anticipated that there would no longer be a requirement for phosphate for high-affinity binding to the Grb7-SH2 domain. Figure 3B shows a series of binding curves measured for peptides **2** and **3** in a range of phosphate concentrations. As

DOI: 10.1021/acs.jmedchem.5b00609
J. Med. Chem. XXXX, XXX, XXX−XXX

expected, the highest affinity measurement for peptide **2** binding to Grb7-SH2 was observed in the absence of phosphate in the buffer (K_D = 3.9 μM) and, with increasing concentrations of phosphate in the buffer the binding was reduced. The affinity of peptide **2** was determined at K_D = 31.1 μM in 50 mM phosphate and K_D = 77.3 μM in 350 mM phosphate-containing buffer. Likewise, the affinity of peptide **3** was lowered to K_D = 6.6 μM in 50 mM phosphate-containing buffer (Table 2; SPR sensorgrams provided as Supporting Information). This was in stark contrast with peptide **1** binding of K_D = 2.9 and 2.6 μM at high phosphate concentrations (Table 2; SPR sensorgrams provided as Supporting Information). Thus, the cmF and cF substitutions successfully enhance peptide binding to the Grb7-SH2 domain, effectively acting as a substitute for phosphate in the pY binding site.

Cyclic Peptides 2 and 3 Are Specific for the Grb7-SH2 Domain over Other Closely Related SH2 Domains. SPR was further utilized to determine whether peptides **2** and **3** retain specificity for the Grb7-SH2 domain over closely related SH2 domains (Grb2-SH2 domain (34% identity) and Grb10-SH2 domain (70% identity)). Using the same SPR method, under physiological phosphate concentrations (1 mM phosphate), peptides **2** and **3** displayed low binding affinities for the Grb2-SH2 domain (K_D = 440 and 560 μM, respectively). Peptide **3** also had low affinity binding (K_D = 420 μM) for the Grb10-SH2 domain, whereas binding measurements could not be determined for peptide **2** (Figure 3C; Table 3). Peptide **1** also displayed low affinity for the Grb2-SH2 domain (K_D of 200 μM) and no detectable binding for the Grb10-SH2 domain (Figure 3C; Table 3). Thus, peptides **2** and **3** successfully maintain specificity for Grb7-SH2 over closely related SH2 domains compared with peptide **1** under physiological phosphate conditions.

Table 3. SPR Binding Studies to Determine Specificity of Cyclic Peptides 1, 2, and 3

	affinity dissociation constant[a] (μM)		
protein	1	2	3
Grb7-SH2	18.1 ± 0.1	5.7 ± 0.03	2.1 ± 0.01
Grb2-SH2	200 ± 70	440 ± 70	560 ± 40
Grb10-SH2	No detectable binding	No detectable binding	420 ± 60

[a]K_D was derived from fits to single-site saturation model. Errors are standard errors arising from the fits. SPR specificity experiments were conducted in 20 mM Tris, 1 mM $NaPO_4$, 150 mM NaCl, and 1 mM DTT

Crystal Structure of the Grb7-SH2:Peptide 2 Complex Reveals the Basis for Binding Affinity. To determine the structural basis of the enhanced binding affinity of **2** and **3** for the Grb7-SH2 domain, cocrystallization of the peptides with the Grb7-SH2 domain was pursued. Only the Grb7-SH2:peptide **2** complex gave rise to crystals suitable for diffraction experiments. The best crystal obtained from the PEG/Ion HT screen diffracted to 2.55 Å with the reservoir solution containing 12% w/v PEG3350, 0.05 M sodium HEPES and 1% w/v tryptone (parameters provided in Table 1). The complex crystallized in the $P2_12_12_1$ space group with unit cell dimensions of a = 55.55, b = 68.96, c = 77.12, $\alpha = \beta = \gamma$ = 90 °C. Molecular replacement was used to determine initial phases using a monomer of the apo-Grb7-SH2 domain as a search model (PDB ID: 4WWQ). The data collection and refinement statistics are provided in Table 1 and the coordinates are deposited in the Protein database (PDB ID: 4X6S). The asymmetric unit contains two chains of the Grb7-SH2 domain, both in complex with cyclic peptide **2**. The electron density for the Grb7 chains encompasses residues 424−529 for chain A and 423−529 for chain B. In the peptide binding site, clear electron density is visible for the peptide ligand including density showing the position of the cmF group (Figure 4A).

The Grb7-SH2 domain adopts the canonical $\alpha\beta\beta\beta\beta\alpha$ SH2 domain topology (Figure 4A) with Cα RMSDs of 0.35 and 0.39 for chains A and B, respectively, compared to chain A of the apo-Grb7 SH2 structure. The interchain covalent linkage observed in the apo-Grb7 structure was not present in this complex structure; but the typical Grb7 family dimerization interface was present, centering on F511 (αB8) from each protomer.

Peptide **2** is positioned across the βD strand in both chains, making contacts with residues from the BC, EF, and BG loops, analogously to peptide **1** in the Grb7-SH2:peptide **1** complex structure (PDB ID: 3PQZ; Figure 4B). Peptide **2** has a Cα RMSD of 0.16 between the two chains in the asymmetric unit, and 0.27 and 0.21 for chains A and B, respectively, compared to peptide **1** chain L across the 11 amino acid residues.

The peptide **2** residues G4, D6, and N7 display the highest level of similarity between the two peptides, with these residues forming the main binding interface with the Grb7-SH2 domain via electrostatic and van der Waals (vdW) interactions (Figure 4B). The F2 and F9 aromatic rings form hydrophobic interactions with the Grb7-SH2 domain surface and the G4 backbone carbonyl forms H-bonding interactions with the Arg438 (αA2) side chain that are equivalent to those seen in the Grb7-SH2:peptide **1** complex structure. In contrast, the flexible solvent exposed residues (W1, E3, T8, and C11) adopt varied rotamer conformations compared with those in peptide **1**.

As predicted, the cmF residue in peptide **2** probes the pY binding pocket of Grb7 mediating additional interactions to those made by peptide **1**. The cmF group is oriented slightly differently between the two chains with an approximate 11° twist at the Cβ position. The average temperature factor of the cmF residue in the two chains, 47 Å^2 for chain A and 52 Å^2 for chain B, is higher than the average temperature factor for the peptide chains, 43 Å^2 for chain A and 49 Å^2 for chain B, suggesting the phosphotyrosine mimetic is relatively mobile compared to the peptide as a whole. This shift between the two cmF groups slightly alters the H-bond network with BC loop residues in the pY binding pocket, but essentially the same contacts are made in chains A and B (Figure 4C and D). The cmF carboxylate O_1 forms H-bond or vdW (where the distance is slightly long for H-bond formation) contacts with the Ser460 (βB7) side chain and the backbone amides of Gln461 (BC1) and Arg462 (BC2), similarly to the mode of interaction seen in the sulfate containing Grb7-SH2 domain structure (PDB ID: 2QMS). The cmF O_2 forms H-bond or vdW interactions with residues at the base of the pY binding pocket including the Arg438 (αA2) guanidinium side chain and bipartite interactions with the Arg458 (βB5) guanidinium group. These are the same amino acids that were observed to bind to malonate; however, the cmF O_2 interaction with Arg438 (αA2) is via the δNH group (since the ωNH_2 groups extends to the G4 backbone carbonyl in peptide **2**). In both chains the BC loop is consistently held in the closed conformation for peptide binding, similarly to the sulfate and malonate-bound Grb7-SH2 structures.

DOI: 10.1021/acs.jmedchem.5b00609
J. Med. Chem. XXXX, XXX, XXX−XXX

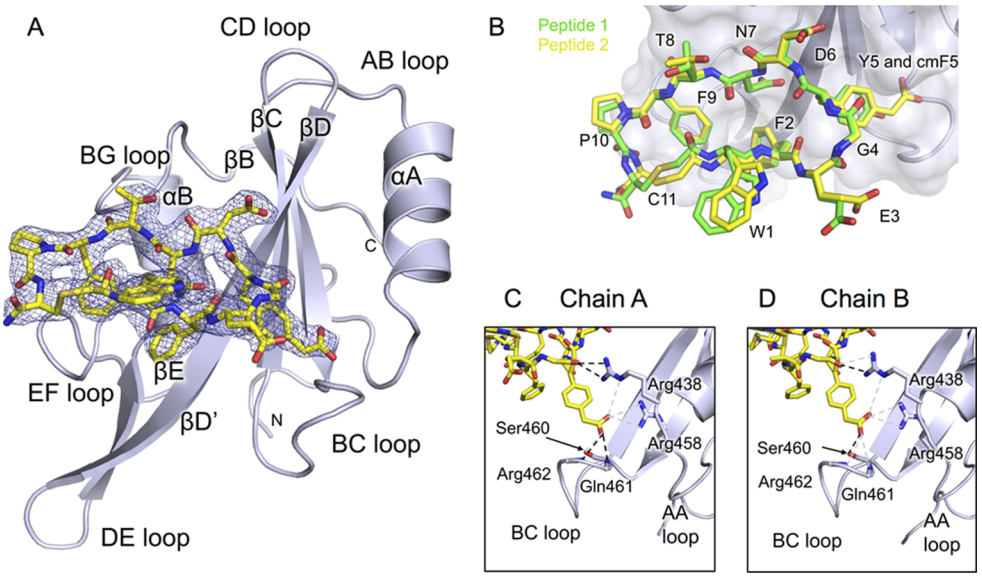

Figure 4. Structure of the Grb7-SH2:peptide **2** complex. (A) Structure of Grb7 SH2 (blue-white cartoon) in complex with peptide **2** (yellow sticks) (PDB ID: 4X6S). 2Fo-Fc map surrounding peptide **2** shown contoured at 1.2σ. (B) Structural overlay of peptide **2** (yellow) and peptide **1** (green) from PDB ID: 3PQZ. Grb7 SH2 shown as blue-white surface representation. (C–D) Close-up of the pY binding pocket of chain A and chain B. Key amino acids are shown as sticks and hydrogen bonds as black dashed lines (or gray if close to being defined as a hydrogen bond).

The crystal structure also reveals that the basis for peptide **2** specificity for the Grb7-SH2 domain is the same as previously reported for peptide **1**.[31] Critical interactions are made with the nonconserved residue Leu481 (βD6) that is known to play a central role in Grb7 binding specificity.[36] The peptide **2** N7 side chain carbonyl and amine groups form bipartate hydrogen bonds with Grb7 Leu481 backbone amino and carbonyl groups, respectively. This positions the peptide such that the aromatic rings of both cmF5 and F2 form van der Waals interactions against the Leu481 side chain that could not occur in other Grb-SH2 domains. Another interaction between peptide **2** and Grb7 that may contribute to binding specificity is a hydrogen bond between the P10 carbonyl group and the nonconserved Grb7 Gln499 (EF4) side chain amine. In addition, due to the subtle effects of shape complementarity, van der Waals contributions to binding specificity are also likely to be at play in the same way as for peptide **1**. Overall, it can be seen that the incorporation of the cmF group in peptide **2** does not negatively impact on the molecular interactions that underlie specificity of binding to the Grb7-SH2 domain.

Peptides 2 and 3 Represent Improved Inhibitors of the Grb7-SH2 Domain. The cmF group has thus successfully been utilized as a pY group replacement, effecting the interactions with the Grb7-SH2 domain similar to those previously observed for sulfate and malonate binding. Although structural data has not yet been obtained for the Grb7-SH2:peptide **3** complex, the cF group in peptide **3** likely makes similar contacts in the pY binding site. As well as providing enhanced binding affinity through direct electrostatic and hydrogen bond contributions, it is possible that the BC loop stabilization also contributes to peptide binding through subtle adjustments to the peptide binding site. The structure helps to explain the increased binding affinity of peptides **2** and **3** over peptide **1** under physiological phosphate concentrations as well as competition for peptide binding by phosphate at higher concentrations.

DISCUSSION

The role of Grb7 in cancer progression through migratory and proliferative signaling, and its overexpression in a myriad of cancers, has highlighted Grb7 as a viable target for developing novel anticancer agents.[2,3,17] Initial success has been made with the discovery of the cyclic nonphosphorylated peptide **1**, with cell-permeable forms inhibiting cell migration, invasion, proliferation, and colony formation in HER2+ and TNBC cell lines.[2,3,9] To further the potential of peptide **1** in therapeutic development, derivatives of this peptide need to be designed, synthesized, and characterized.

The current study has identified two new cyclic derivatives, peptides **2** and **3**, with enhanced affinity for the Grb7-SH2 domain compared with peptide **1**. The introduction of the cmF and cF moieties at the Y5 position of peptide **1** was inspired by the observation of a malonate positioned in the pY binding site of the apo-Grb7-SH2 domain crystal structure. The target cyclic peptides were successfully prepared via solid-phase peptide synthesis and binding studies using SPR determined that peptide **2** improves binding 3-fold and peptide **3** 9-fold for the Grb7-SH2 domain compared with peptide **1**. Importantly, these measurements are in the presence of 1 mM phosphate, which reflects a physiological phosphate concentration.[37] Furthermore, peptides **2** and **3** show greater than 75-fold higher binding for the Grb7-SH2 domain over the closely related Grb2- and Grb10-SH2 domains under the same conditions. While these studies were not conducted on the full-length Grb proteins, it is anticipated that this specificity will be retained in the cellular environment. In studies conducted to test the binding of peptides **1**, **2**, and **3** to full-length Grb7 (using the same SPR strategy as for the SH2 domain alone) we were able to confirm binding affinities in the micromolar range (peptides **2** and **3** binding with approximately 4-fold and 8-fold higher affinity than peptide **1**, respectively), though the instability of full-length Grb7 over time prevented the determination of accurate values for peptide binding (the data and a description of these experiments are supplied as Supporting Information). This shows, however, that the inhibitor peptides do bind to the

DOI: 10.1021/acs.jmedchem.5b00609
J. Med. Chem. XXXX, XXX, XXX–XXX

Grb7 in the context of the whole protein and not just to the isolated SH2 domain.

Our structural studies confirm that the cmF group of peptide **2** reaches into the Grb7 pY-binding pocket mediating a combination of interactions previously observed in the malonate- and sulfate-bound Grb7-SH2 domain structures, effectively holding the BC loop in a closed and favorable conformation for peptide binding. The cmF is thus a successful pY mimetic for Grb7-SH2 inhibitors. Structural data have not been obtained for the Grb7-SH2:peptide **3** complex, so it is not yet known how the cF group interacts in the pY-binding pocket to effect the higher affinity interaction. In the case of the cF group, it is shorter than cmF by one methylene group and seemingly less ideal for placement in the binding site from inspection of Y in peptide **1** and malonate when bound to the Grb7-SH2 domain (Figure 1A). Nevertheless, this study has shown it makes additional productive interactions with Grb7-SH2 domain target and is also a successful pY mimetic for Grb7-SH2 inhibitors.

The cmF group has been utilized as a pY mimetic in previous studies of SH2 inhibition.[33,38,39] Incorporation of the cmF group to Src SH2 and Grb2-targeted peptides improved binding >2-fold and from undetectable to low μM binding, respectively, compared to Y alone.[33,38,40] It is the case, however, that cmF derivatives have reduced binding compared to their pY peptide counterparts: 940-fold for Src, 50-fold for Grb2, and 467-fold for a $p56^{lck}$ directed cmF peptide.[33,38,39] It has been determined that the phosphate group can contribute up to half the total binding energy to SH2 domain binding.[41] Thus, the cmF group only partially mimics the pY group as may be expected for a single dicarboxylic acid with less capacity for H-bond formation than a phosphate. A further increase in binding affinity may be achieved with the use of a higher valency pY mimetic or with the use of a protected phosphate group as developed by McMurray et al.[16] This study represents the first time, to our knowledge, that the cF group has been incorporated and tested as a pY mimetic for targeting an SH2 domain binding pocket. The cF group has previously been substituted for the Y+3 phenylalanine in Src targeting peptides. This single substitution showed a 180-fold improvement in inhibiting the substrate $polyGlu_4Tyr$ compared to the parent phenylalanine containing peptide.[34]

The current study has demonstrated that peptides **2** and **3** maintain specificity for Grb7-SH2 under physiological conditions. While the cF and cmF groups confer greater affinity for the Grb7-SH2 domain, binding to Grb2 and Grb10 is only marginally affected. Peptides **2** and **3**, in fact, showed decreased binding to Grb2-SH2 compared to peptide **1**, though peptide **3** showed a detectable interaction with the Grb10-SH2 domain where peptides **1** and **2** had shown no interaction. This is similar to the effect observed upon addition of phosphate to the buffer on peptide **1** binding. While peptide **1** binding to Grb7-SH2 domain was greatly enhanced in 100 mM phosphate, binding to Grb10-SH2 and Grb2-SH2 domain was either not enhanced or only marginally enhanced.[24] Grb10-SH2 possesses a significant sequence identity of ~70% with Grb7-SH2, and although Grb2 possesses a low sequence identity of ~34%, the SH2 domain shares the same substrate as Grb7, the ErbB2 receptor, and thus recognizes the same pYXN interaction motif. Furthermore, the amino acid side chains shown to be important for binding to the cmF group (of Ser460 (βB7), Arg438 (αA2), Arg458 (βB5)) are conserved between the Grb7 family members and Grb2. Specificity of cyclic peptides **2** and **3** for the Grb7-SH2 domain is thus likely to occur via other more subtle interactions across the surface of the protein where it makes contact across the βD strand, BG loop, and EF loop as previously observed for peptide **1**.[31]

In the development of SH2 domain inhibitors it is an achievement to develop a specific inhibitor suitable for cellular studies due to the large number of SH2 domains that exist in the cell with similar substrate interactions. Peptide **1** was the first molecule to be discovered with specificity for Grb7, but its affinity depends upon the presence of phosphate ions. Other peptides and small molecules have been discovered that bind to Grb7 but have not been shown to possess binding specificity.[42−44] This study thus reveals an important new class of inhibitor that is specific for the Grb7-SH2 domain under physiological conditions. Future work will focus on improving the inhibitor affinity. With a K_D = 2.1 μM binding affinity for the Grb7-SH2 domain, cyclic peptide **3** represents an improvement on peptide **1**, but still higher affinities are required for its therapeutic use. The structural information obtained for the Grb7-SH2:peptide **2** complex will facilitate the design of further modifications for improvement of this first generation inhibitor of Grb7. These may include additional hydrogen bonding functionalities and rigidification of the peptide backbone as have previously shown to be successful in peptide inhibitor design.[26,45] The effective synthesis and characterization of cyclic peptides **2** and **3** thus represents an important step toward a potent Grb7-SH2 domain inhibitor that will be used as a tool both for better understanding the downstream effects of Grb7 inside cells and for future potential therapeutic use in the treatment of HER2+ and TNBC.

METHODS

Protein Expression and Purification. The pGex2T plasmids containing the SH2 domain inserts of Grb2 (encoding residues 58−160), Grb7 (encoding residues 415−532) and Grb10 (encoding residues 471−594) were kindly provided by Roger Daly. The SH2 domains were expressed as GST fusion proteins in *Escherichia coli* strain BL21(DE3)pLysS and purified using glutathione affinity chromatography and size exclusion chromatography as described previously.[24,30] To obtain Grb7-SH2 domain alone for crystallization experiments, the GST tag was cleaved off with thrombin following glutathione affinity chromatography, and further purified with cation exchange and size exclusion chromatography as also described previously.[30] The GST alone, used as a control for SPR, was expressed from the pGex2T plasmid (GE Healthcare) and purified similarly to the GST-Grb proteins excluding size exclusion chromatography. The final concentrations of GST, GST-Grb7-SH2, GST-Grb2-SH2, GST-Grb10-SH2, and Grb7-SH2 were determined spectrophotometrically at A_{280} using extinction coefficients of 42860, 51340, 58330, 49850, and 8480 M^{-1} cm^{-1}, respectively.[46]

Preparation of Fmoc-cmF(methyl ester)-OH. Fmoc-cmF-(OMe)-OH **4** was synthesized from Boc-cmF(OMe)-O*t*Bu that was in turn prepared using a procedure previously reported by Tilley et al.[35] Briefly, Boc-cmF(OMe)-O*t*Bu (108 mg, 0.27 mmol, 1 equiv) was treated with an acidic cocktail comprising a 90:5:5 v/v/v mixture of TFA:triisopropylsilane:H_2O (2 mL) and allowed to stir at rt for 3 h before removal of the solution *in vacuo*. The crude product was used in the next step without further purification. A solution of the resulting amino acid in a 2:1 v/v mixture of 1,4-dioxane/sat. aq. $NaHCO_3$ solution (3 mL) was treated with Fmoc-OSu (102 mg, 0.3 mmol, 1.1 equiv) and allowed to stir at rt for 16 h. The resulting mixture was poured onto water, and acidified to pH 1−2 with 1 M HCl, extracted with EtOAc (3 times), dried (Na_2SO_4), and concentrated *in vacuo*. The crude product was purified by column chromatography (1:1 v/v EtOAc/hexanes +1% to 3% MeOH), to afford Fmoc-cmF(OMe)-OH **4** as a colorless oil (107 mg, 86%). ^1H NMR (d_6-acetone, 400 MHz) δ

DOI: 10.1021/acs.jmedchem.5b00609
J. Med. Chem. XXXX, XXX, XXX−XXX

(ppm) 7.86 (d, J = 7.20 Hz, 2H), 7.70−7.63 (m, 2H), 7.45−7.20 (m, 8H), 6.72 (d, J = 8.34 Hz), 4.60−4.50 (m, 1H), 4.38−4.16 (m, 3H), 3.65−3.59 (m, 5H), 3.27 (dd, J = 4.78, 14.03 Hz, 1H), 3.06 (dd, J = 9.56, 14.03 Hz, 1H); ^{13}C NMR (d_6-acetone, 100 MHz) δ (ppm) 173.3, 172.3, 156.8, 144.9, 142.0, 137.0, 133.8, 130.2, 130.1, 128.5, 127.9, 126.2, 120.8, 67.2, 56.1, 51.9, 47.9, 40.9, 37.7. HRMS: ($M_{expected}$ = 459.1682 g/mol, $M_{measured}$ = 459.1682 g/mol).

Synthesis of Peptides 1, 2, and 3. Peptide **2** (cyclo-(CH_2CO-WFEG**cmF**DNTFPC)-$CONH_2$) was synthesized on a 0.1 mmol scale using standard Fmoc-chemistry on Rink amide resin (0.7 mmol/g). Commercially available amino acids (3.1 equiv with respect to the resin loading), HBTU (3.0 equiv with respect to the resin loading), HOBt (3.0 equiv to resin loading), and DIPEA (4.5 equiv to resin loading) were dissolved in DMF (3 mL) and added to the resin with shaking for 45 min. These reactions were repeated twice to ensure complete coupling. Fmoc-cmF(OMe)-OH **4** was only coupled once in slight excess of 1.3 equiv to resin loading, along with HBTU (1.3 equiv with respect to the resin loading), HOBt (1.3 equiv to resin loading), and DIPEA (∼2 equiv to resin loading) in DMF (2 mL). After removal of the terminal Fmoc protecting group on the resin-bound peptide through the treatment with 20 vol % piperidine in DMF, the resin was treated with chloroacetic anhydride (1 mmol) and DIPEA (0.1 mmol) in DMF (2 mL) to afford a chloroacetyl-capped N-terminus. The resin was subsequently washed with DMF, CH_2Cl_2, and Et_2O and dried. Cleavage was performed on 0.15 mmol of the resin by treating the resin with a cleavage solution comprising distilled water (2.5% v/v), triisopropylsilane (2.5% v/v), and ethanedithiol (0.5% v/v) in TFA (9.45 mL) for 1.5 h. The TFA was then evaporated under a stream of N_2 and the peptide precipitated by addition of cold Et_2O. The precipitate was filtered and redissolved in H_2O/CH_3CN (1:1) for lyophilization.

Thioether formation was effected by dissolving the peptide (2 mg/mL concentration) in 50 mM NH_4HCO_3 solution (made up in 1:1 v/v CH_3CN/H_2O), at pH 8.0, for 1.5 h at room temperature. The cyclized peptide was then purified using reverse-phase HPLC. Hydrolysis of the methyl ester protecting group on the side chain of the cmF residue was carried out by dissolving the peptide (1 mg/mL concentration) in 10−11 mM NaOH solution (0.5 mL of CH_3CN in 6.5 mL of H_2O), at pH 8.0−9.0, for 30 h at room temperature. After final purification (to ≥95% purity based on LC) the peptide mass was verified by ion-trap mass spectrometry ($M_{expected}$ $(C_{69}H_{81}N_{14}O_{20}S)^-$ = 1457.6; $M_{measured}$ $(C_{69}H_{81}N_{14}O_{20}S)^-$ = 1457.6; $M_{expected}$ $(C_{69}H_{81}N_{14}O_{20}S)^{2-}$ = 728.3; $M_{measured}$ $(C_{69}H_{81}N_{14}O_{20}S)^{2-}$ = 728.5).

The synthesis of cyclic peptide **3** (cyclo-(CH_2CO-WFEG**cF**DNTFPC)-$CONH_2$) was carried out using a similar protocol to that for peptide **2** by Wuxi Nordisk Biotech (China) to >95% purity based on LC-MS. In this case, the Fmoc-protected cF residue (Fmoc-*p*-carboxyphenylalanine(O*t*Bu)-OH) was commercially available (Chem-Impex). After purification using reverse-phase HPLC the peptide mass was verified by ion-trap mass spectrometry ($M_{expected}$ $(C_{68}H_{79}N_{14}O_{20}S)^-$ = 1443.6; $M_{measured}$ $(C_{68}H_{79}N_{14}O_{20}S)^-$ = 1443.9; $M_{expected}$ $(C_{68}H_{79}N_{14}O_{20}S)^{2-}$ = 721.8; $M_{measured}$ $(C_{68}H_{79}N_{14}O_{20}S)^{2-}$ = 721.6).

Peptide **1** (cyclo-(CH_2CO-WFEGYDNTFPC)-amide) was prepared as described previously.[21] The final concentrations of peptides **1**, **2**, and **3** were determined spectrophotometrically at A_{280} using extinction coefficients of 6990 M^{-1} cm^{-1} and 5809 M^{-1} cm^{-1}, respectively, with the extinction coefficient for the latter two calculated using the DirectDetect (Millipore) system.

Protein Crystallization, X-ray Diffraction Data Collection, and Structure Determination. Apo-Grb7-SH2 crystals were prepared and data collected as previously described.[27] The diffraction images were indexed and integrated in the space group $P6_3$ using IMOSFLM scaled with SCALA from the CCP4 suite and cut to a high resolution limit of 1.80 Å.[47−49] 5% of the total reflections were randomly assigned as an R_{free} set using UNIQUEIFY (CCP4 suite) and subsequently excluded from refinement. Molecular replacement was performed using MOLREP with a monomer from the previous Grb7-SH2 domain apo structure used as a search model (PDB ID: 2QMS).[21,50] Rounds of structure refinement and model building were carried out using COOT, PHENIX, and REFMAC5.[51−53] Solvent molecules were automatically added during refinement, and then manually edited in COOT. The final apo-Grb7-SH2 model had an overall R_{work} of 17.60% and an R_{free} of 20.63%.

The Grb7-SH2: peptide **2** complex was formed using 10 mg/mL protein in a 1:1.5 molar ratio of protein:peptide. Crystals were obtained using 2 μL hanging drops composed of 1:1 protein: reservoir with the reservoir solution containing 0.05 M HEPES, pH 7.0, 1% tryptone and 12% PEG3350 from the Hampton screen PEG/Ion HT Screen. Harvestable crystals were soaked in 15% v/v glycerol/mother liquor as a cryoprotectant and flash frozen in liquid nitrogen prior to data collection held in a stream of nitrogen gas at 100 K. Diffraction data were collected using the microfocus beamline (MX2) at the Australian Synchrotron at a wavelength of 0.954 Å using an ADSC Quantum 315r detector and BLU-ICE software for data acquisition.[54] Images were recorded with an oscillation angle of 1° and exposure time of 3 s. The diffraction images were integrated and scaled with the software pipeline XIA2, with the data restricted to a high-resolution limit of 2.55 Å.[55] 5% of the total reflections were randomly assigned as an R_{free} set and excluded from refinement. Phaser was used for molecular replacement with one chain of the apo Grb7-SH2 domain structure (PDB ID: 4WWQ) used as a search model.[56] Subsequent model building and refinement rounds occurred as for the apo Grb7 SH2 structure. The peptide **2** restraint files were generated using phenix.elbow from SMILES strings.[57] The final Grb7 SH2:peptide **1** model had an overall R_{work} of 21.17% and an R_{free} of 25.81%.

MOLPROBITY was used to assess the quality of the final structures, and figures were generated using PyMOL.[58] The data collection, processing, and refinement statistics for both structures are provided in Table 1.

Binding Studies Using Surface Plasmon Resonance. Experiments were conducted on a BIAcore T100 using BIAcore CM5 series S sensor chips as previously reported.[22] The immobilization buffer consisted of 50 mM $NaPO_4$, 150 mM NaCl, and 1 mM DTT (pH 7.4). Polyclonal anti-GST antibody was immobilized on the reference and active flow cells using amine coupling of the antibody to the surface of the chip (GE Healthcare GST capture kit). For this, the sensor chip was activated with 1-ethyl-3-(3-(dimethylamino)propyl)-carbodiimide hydrochloride and *N*-hydroxysuccinimide, then polyclonal anti-GST antibody (at 30 μg/mL) in 10 mM sodium acetate pH 5.0 injected over the chip surface at 5 μL/min for 7 min. The flow cells were then blocked with 1 M ethanolamine, resulting in anti-GST antibody immobilization levels between 2755 RU and 6692 RU.

GST alone was immobilized on the reference flow cell and the GST-fusion proteins of Grb2-SH2, Grb7-SH2, and Grb10-SH2 immobilized on the active flow cells so that binding in the four flow cells could be simultaneously assessed. GST, Grb7-SH2, Grb2-SH2, and Grb10-SH2 (all at 0.7−0.9 μM in immobilization buffer) were injected over the corresponding flow cells for 7 min at 5 μL/min with 486−1272 RU, 767−1521 RU, 800−972 RU, and 811−1065 RU immobilized, respectively. Triplicate or duplicate samples of peptide were injected for 60 s at 30 μL/min, with 300−600 s dissociation in a range of buffers as described in the main text. The data were analyzed using Scrubber2.0 (BioLogic Software, Campbell, ACT, Australia) and SigmaPlot v 12.0 (Systat Software, Inc., Chicago, IL, USA) to determine K_D values.

■ ASSOCIATED CONTENT

Supporting Information

The Supporting Information is available free of charge on the ACS Publications website at DOI: 10.1021/acs.jmedchem.5b00609.

Validation of compounds prepared for this study are provided, as are SPR sensorgrams used for K_D determination. **I**. Supporting Information and Methods. **II**. ^{1}H and ^{13}C NMR spectra of Fmoc-cmF(OMe)-OH **4**. **III**. MS for Fmoc-cmF(OMe)-OH **4**. **IV**. LC chromatogram for peptide **2**. **V**. MS for peptide **2**. **VI**. LC

DOI: 10.1021/acs.jmedchem.5b00609
J. Med. Chem. XXXX, XXX, XXX−XXX

chromatogram for peptide **3**. **VII**. MS for peptide **3**. **VIII**. SPR sensorgrams for peptides **1**, **2**, and **3** binding to the SH2 domains of Grb2, Grb7, and Grb10. **IX**. SPR sensorgrams and equilibrium binding curves for peptides **1**, **2**, and **3** binding to full-length Grb7 and Grb7-SH2 (PDF)

Accession Codes

Coordinates and structure factors have been deposited in the PDB with accession numbers 4WWQ for apo-Grb7-SH2 and 4X6S for Grb7-SH2:**2** complex.

AUTHOR INFORMATION

Corresponding Author

*E-mail: jackie.wilce@monash.edu. Phone: + 613 9902 9226. Fax: + 613 9902 9500.

Notes

The authors declare no competing financial interest.

ACKNOWLEDGMENTS

We wish to thank all the beamline staff at the MX2 at the Australian Synchrotron, Victoria, Australia where the diffraction data were collected. This work was supported by a grant from the National Health and Medical Research Council awarded to J.A.W., P.P., and S.C.P., a National Health and Medical Research Senior Research Fellowship awarded to M.C.J.W. as well as the Victorian Government's Operational Infrastructure Support Program.

ABBREVIATIONS

cmF, carboxymethylphenylalanine; cF, carboxyphenylalanine; Grb, growth factor receptor bound protein; HER2, human epidermal growth factor receptor 2; K_D, equilibrium dissociation constant; LC, liquid chromatography; MLA, malonic acid; MS, mass spectrometry; PH, pleckstrin homology; pY, phosphotyrosine; RA, ras-associating; RU, response units; SH2, src homology 2; SPR, surface plasmon resonance; TNBC, triple negative breast cancer

REFERENCES

(1) Hanahan, D.; Weinberg, R. A. Hallmarks of cancer: the next generation. *Cell* **2011**, *144*, 646−74.
(2) Pradip, D.; Bouzyk, M.; Dey, N.; Leyland-Jones, B. Dissecting GRB7-mediated signals for proliferation and migration in HER2 overexpressing breast tumor cells: GTP-ase rules. *Am. J. Cancer Res.* **2013**, *3*, 173−95.
(3) Giricz, O.; Calvo, V.; Pero, S. C.; Krag, D. N.; Sparano, J. A.; Kenny, P. A. GRB7 is required for triple-negative breast cancer cell invasion and survival. *Breast Cancer Res. Treat.* **2012**, *133*, 607−15.
(4) Bai, T.; Luoh, S. W. GRB-7 facilitates HER-2/Neu-mediated signal transduction and tumor formation. *Carcinogenesis* **2007**, *29*, 473−479.
(5) Chu, P. Y.; Li, T. K.; Ding, S. T.; Lai, I. R.; Shen, T. L. EGF-induced Grb7 recruits and promotes Ras activity essential for the tumorigenicity of Sk-Br3 breast cancer cells. *J. Biol. Chem.* **2010**, *285*, 29279−85.
(6) Nencioni, A.; Cea, M.; Garuti, A.; Passalacqua, M.; Raffaghello, L.; Soncini, D.; Moran, E.; Zoppoli, G.; Pistoia, V.; Patrone, F.; Ballestrero, A. Grb7 upregulation is a molecular adaptation to HER2 signaling inhibition due to removal of Akt-mediated gene repression. *PLoS One* **2010**, *5*, e9024.
(7) Pero, S. C.; Shukla, G. S.; Cookson, M. M.; Flemer, S., Jr.; Krag, D. N. Combination treatment with Grb7 peptide and Doxorubicin or Trastuzumab (Herceptin) results in cooperative cell growth inhibition in breast cancer cells. *Br. J. Cancer* **2007**, *96*, 1520−5.
(8) Han, D. C.; Guan, J. L. Association of focal adhesion kinase with Grb7 and its role in cell migration. *J. Biol. Chem.* **1999**, *274*, 24425−30.
(9) Lim, R. C.; Price, J. T.; Wilce, J. A. Context-dependent role of Grb7 in HER2+ve and triple-negative breast cancer cell lines. *Breast Cancer Res. Treat.* **2014**, *143*, 593−603.
(10) Tanaka, S.; Pero, S. C.; Taguchi, K.; Shimada, M.; Mori, M.; Krag, D. N.; Arii, S. Specific peptide ligand for Grb7 signal transduction protein and pancreatic cancer metastasis. *J. Natl. Cancer Inst.* **2006**, *98*, 491−8.
(11) Ramsey, B.; Bai, T.; Hanlon Newell, A.; Troxell, M.; Park, B.; Olson, S.; Keenan, E.; Luoh, S. W. GRB7 protein over-expression and clinical outcome in breast cancer. *Breast Cancer Res. Treat.* **2011**, *127*, 659−69.
(12) Nadler, Y.; Gonzalez, A. M.; Camp, R. L.; Rimm, D. L.; Kluger, H. M.; Kluger, Y. Growth factor receptor-bound protein-7 (Grb7) as a prognostic marker and therapeutic target in breast cancer. *Ann. Oncol.* **2010**, *21*, 466−73.
(13) Stein, D.; Wu, J.; Fuqua, S. A.; Roonprapunt, C.; Yajnik, V.; D'Eustachio, P.; Moskow, J. J.; Buchberg, A. M.; Osborne, C. K.; Margolis, B. The SH2 domain protein GRB-7 is co-amplified, overexpressed and in a tight complex with HER2 in breast cancer. *EMBO J.* **1994**, *13*, 1331−40.
(14) Fiddes, R. J.; Campbell, D. H.; Janes, P. W.; Sivertsen, S. P.; Sasaki, H.; Wallasch, C.; Daly, R. J. Analysis of Grb7 recruitment by heregulin-activated erbB receptors reveals a novel target selectivity for erbB3. *J. Biol. Chem.* **1998**, *273*, 7717−24.
(15) Margolis, B.; Silvennoinen, O.; Comoglio, F.; Roonprapunt, C.; Skolnik, E.; Ullrich, A.; Schlessinger, J. High-efficiency expression/cloning of epidermal growth factor-receptor-binding proteins with Src homology 2 domains. *Proc. Natl. Acad. Sci. U. S. A.* **1992**, *89*, 8894−8.
(16) McMurray, J. S.; Mandal, P. K.; Liao, W. S.; Klostergaard, J.; Robertson, F. M. The consequences of selective inhibition of signal transducer and activator of transcription 3 (STAT3) tyrosine705 phosphorylation by phosphopeptide mimetic prodrugs targeting the Src homology 2 (SH2) domain. *Jak-Stat* **2012**, *1*, 263−347.
(17) Kraskouskaya, D.; Duodu, E.; Arpin, C. C.; Gunning, P. T. Progress towards the development of SH2 domain inhibitors. *Chem. Soc. Rev.* **2013**, *42*, 3337−70.
(18) Zhou, S.; Shoelson, S. E.; Chaudhuri, M.; Gish, G.; Pawson, T.; Haser, W. G.; King, F.; Roberts, T.; Ratnofsky, S.; Lechleider, R. J.; Neel, B. G.; Birge, R. B.; Fajardo, J. E.; Chou, M. M.; Hanafusa, H.; Schaffhausen, B.; Cantley, L. C. SH2 domains recognize specific phosphopeptide sequences. *Cell* **1993**, *72*, 767−778.
(19) Pero, S. C.; Daly, R. J.; Krag, D. N. Grb7-based molecular therapeutics in cancer. *Expert Rev. Mol. Med.* **2003**, *5*, 1−11.
(20) Pero, S. C.; Oligino, L.; Daly, R. J.; Soden, A. L.; Liu, C.; Roller, P. P.; Li, P.; Krag, D. N. Identification of novel non-phosphorylated ligands, which bind selectively to the SH2 domain of Grb7. *J. Biol. Chem.* **2002**, *277*, 11918−26.
(21) Porter, C. J.; Matthews, J. M.; Mackay, J. P.; Pursglove, S. E.; Schmidberger, J. W.; Leedman, P. J.; Pero, S. C.; Krag, D. N.; Wilce, M. C. J.; Wilce, J. A. Grb7 SH2 domain structure and interactions with a cyclic peptide inhibitor of cancer cell migration and proliferation. *BMC Struct. Biol.* **2007**, *7*, 58.
(22) Gunzburg, M. J.; Ambaye, N. D.; Hertzog, J. T.; del Borgo, M. P.; Pero, S. C.; Krag, D. N.; Wilce, M. C. J.; Aguilar, M.-I.; Perlmutter, P.; Wilce, J. A. Use of SPR to Study the Interaction of G7−18NATE Peptide with the Grb7-SH2 Domain. *Int. J. Pept. Res. Ther.* **2010**, *16*, 177−184.
(23) Spuches, A. M.; Argiros, H. J.; Lee, K. H.; Haas, L. L.; Pero, S. C.; Krag, D. N.; Roller, P. P.; Wilcox, D. E.; Lyons, B. A. Calorimetric investigation of phosphorylated and non-phosphorylated peptide ligand binding to the human Grb7-SH2 domain. *J. Mol. Recognit.* **2007**, *20*, 245−52.
(24) Gunzburg, M. J.; Ambaye, N. D.; Del Borgo, M. P.; Pero, S. C.; Krag, D. N.; Wilce, M. C.; Wilce, J. A. Interaction of the non-phosphorylated peptide G7−18NATE with Grb7-SH2 domain requires phosphate for enhanced affinity and specificity. *J. Mol. Recognit.* **2012**, *25*, 57−67.

DOI: 10.1021/acs.jmedchem.5b00609
J. Med. Chem. XXXX, XXX, XXX−XXX

(25) Eck, M. J.; Shoelson, S. E.; Harrison, S. C. Recognition of a high-affinity phosphotyrosyl peptide by the Src homology-2 domain of p56lck. *Nature* **1993**, *362*, 87−91.
(26) Burke, T. R., Jr.; Lee, K. Phosphotyrosyl mimetics in the development of signal transduction inhibitors. *Acc. Chem. Res.* **2003**, *36*, 426−33.
(27) Ambaye, N. D.; Gunzburg, M. J.; Traore, D. A. K.; Del Borgo, M. P.; Perlmutter, P.; Wilce, M. C. J.; Wilce, J. A. Preparation of crystals for characterizing the Grb7 SH2 domain before and after complex formation with a bicyclic peptide antagonist. *Acta Crystallogr., Sect. F: Struct. Biol. Commun.* **2014**, *70*, 182−186.
(28) Stein, E. G.; Ghirlando, R.; Hubbard, S. R. Structural basis for dimerization of the Grb10 Src homology 2 domain. Implications for ligand specificity. *J. Biol. Chem.* **2003**, *278*, 13257−64.
(29) Depetris, R. S.; Hu, J.; Gimpelevich, I.; Holt, L. J.; Daly, R. J.; Hubbard, S. R. Structural basis for inhibition of the insulin receptor by the adaptor protein Grb14. *Mol. Cell* **2005**, *20*, 325−33.
(30) Porter, C. J.; Wilce, M. C.; Mackay, J. P.; Leedman, P.; Wilce, J. A. Grb7-SH2 domain dimerisation is affected by a single point mutation. *Eur. Biophys. J.* **2005**, *34*, 454−60.
(31) Ambaye, N. D.; Pero, S. C.; Gunzburg, M. J.; Yap, M.; Clayton, D. J.; Del Borgo, M. P.; Perlmutter, P.; Aguilar, M. I.; Shukla, G. S.; Peletskaya, E.; Cookson, M. M.; Krag, D. N.; Wilce, M. C.; Wilce, J. A. Structural basis of binding by cyclic nonphosphorylated peptide antagonists of Grb7 implicated in breast cancer progression. *J. Mol. Biol.* **2011**, *412*, 397−411.
(32) Waksman, G.; Shoelson, S. E.; Pant, N.; Cowburn, D.; Kuriyan, J. Binding of a high affinity phosphotyrosyl peptide to the Src SH2 domain: crystal structures of the complexed and peptide-free forms. *Cell* **1993**, *72*, 779−90.
(33) Burke, T. R., Jr.; Luo, J.; Yao, Z. J.; Gao, Y.; Zhao, H.; Milne, G. W.; Guo, R.; Voigt, J. H.; King, C. R.; Yang, D. Monocarboxylic-based phosphotyrosyl mimetics in the design of GRB2 SH2 domain inhibitors. *Bioorg. Med. Chem. Lett.* **1999**, *9*, 347−52.
(34) Wang, W.; Ramdas, L.; Sun, G.; Ke, S.; Obeyesekere, N. U.; Budde, R. J.; McMurray, J. S. Cyclic peptides incorporating 4-carboxyphenylalanine and phosphotyrosine are potent inhibitors of pp60(c-) (src). *Biochemistry* **2000**, *39*, 5221−8.
(35) Tilley, J. W.; Sarabu, R.; Wagner, R.; Mulkerins, K. Preparation of carboalkoxyalkylphenylalanine derivatives from tyrosine. *J. Org. Chem.* **1990**, *55*, 906−910.
(36) Janes, P. W.; Lackmann, M.; Church, W. B.; Sanderson, G. M.; Sutherland, R. L.; Daly, R. J. Structural determinants of the interaction between the erbB2 receptor and the Src homology 2 domain of Grb7. *J. Biol. Chem.* **1997**, *272*, 8490−7.
(37) Bevington, A.; Mundy, K. I.; Yates, A. J.; Kanis, J. A.; Russell, R. G.; Taylor, D. J.; Rajagopalan, B.; Radda, G. K. A study of intracellular orthophosphate concentration in human muscle and erythrocytes by 31P nuclear magnetic resonance spectroscopy and selective chemical assay. *Clin. Sci.* **1986**, *71*, 729−35.
(38) Gilmer, T.; Rodriguez, M.; Jordan, S.; Crosby, R.; Alligood, K.; Green, M.; Kimery, M.; Wagner, C.; Kinder, D.; Charifson, P.; Hassell, A. M.; Willard, D.; Luther, M.; Rusnak, D.; Sternbach, D. D.; Mehrotra, M.; Peel, M.; Shampine, L.; Davis, R.; Robbins, J.; Patel, I. R.; Kassel, D.; Burkhart, W.; Moyer, M.; Bradshaw, T.; Berman, J. Peptide inhibitors of src SH3-SH2-phosphoprotein interactions. *J. Biol. Chem.* **1994**, *269*, 31711−31719.
(39) Tong, L.; Warren, T. C.; Lukas, S.; Schembri-King, J.; Betageri, R.; Proudfoot, J. R.; Jakes, S. Carboxymethyl-phenylalanine as a replacement for phosphotyrosine in SH2 domain binding. *J. Biol. Chem.* **1998**, *273*, 20238−42.
(40) Yao, Z. J.; King, C. R.; Cao, T.; Kelley, J.; Milne, G. W.; Voigt, J. H.; Burke, T. R., Jr. Potent inhibition of Grb2 SH2 domain binding by non-phosphate-containing ligands. *J. Med. Chem.* **1999**, *42*, 25−35.
(41) Bradshaw, J. M.; Mitaxov, V.; Waksman, G. Investigation of phosphotyrosine recognition by the SH2 domain of the Src kinase. *J. Mol. Biol.* **1999**, *293*, 971−85.
(42) Luzy, J. P.; Chen, H.; Gril, B.; Liu, W. Q.; Vidal, M.; Perdereau, D.; Burnol, A. F.; Garbay, C. Development of binding assays for the SH2 domain of Grb7 and Grb2 using fluorescence polarization. *J. Biomol. Screening* **2008**, *13*, 112−9.
(43) Ambaye, N. D.; Gunzburg, M. J.; Lim, R. C.; Price, J. T.; Wilce, M. C.; Wilce, J. A. Benzopyrazine derivatives: A novel class of growth factor receptor bound protein 7 antagonists. *Bioorg. Med. Chem.* **2011**, *19*, 693−701.
(44) Ambaye, N. D.; Gunzburg, M. J.; Lim, R. C.; Price, J. T.; Wilce, M. C.; Wilce, J. A. The discovery of phenylbenzamide derivatives as Grb7-based antitumor agents. *ChemMedChem* **2013**, *8*, 280−8.
(45) Morlacchi, P.; Robertson, F. M.; Klostergaard, J.; McMurray, J. S. Targeting SH2 domains in breast cancer. *Future Med. Chem.* **2014**, *6*, 1909−26.
(46) Pace, C. N.; Vajdos, F.; Fee, L.; Grimsley, G.; Gray, T. How to measure and predict the molar absorption coefficient of a protein. *Protein Sci.* **1995**, *4*, 2411−23.
(47) Leslie, A. W.; Powell, H. Processing Diffraction Data with Mosflm. In *Evolving Methods for Macromolecular Crystallography*, Read, R.; Sussman, J., Eds.; Springer: Dordrecht, 2007; Vol. *245*, pp 41−51.
(48) Evans, P. Scaling and assessment of data quality. *Acta Crystallogr., Sect. D: Biol. Crystallogr.* **2006**, *62*, 72−82.
(49) Winn, M. D.; Ballard, C. C.; Cowtan, K. D.; Dodson, E. J.; Emsley, P.; Evans, P. R.; Keegan, R. M.; Krissinel, E. B.; Leslie, A. G.; McCoy, A.; McNicholas, S. J.; Murshudov, G. N.; Pannu, N. S.; Potterton, E. A.; Powell, H. R.; Read, R. J.; Vagin, A.; Wilson, K. S. Overview of the CCP4 suite and current developments. *Acta Crystallogr., Sect. D: Biol. Crystallogr.* **2011**, *67*, 235−42.
(50) Vagin, A.; Teplyakov, A. Molecular replacement with MOLREP. *Acta Crystallogr., Sect. D: Biol. Crystallogr.* **2010**, *66*, 22−5.
(51) Emsley, P.; Cowtan, K. Coot: model-building tools for molecular graphics. *Acta Crystallogr., Sect. D: Biol. Crystallogr.* **2004**, *60*, 2126−32.
(52) Murshudov, G. N.; Vagin, A. A.; Dodson, E. J. Refinement of macromolecular structures by the maximum-likelihood method. *Acta Crystallogr., Sect. D: Biol. Crystallogr.* **1997**, *53*, 240−55.
(53) Afonine, P. V.; Grosse-Kunstleve, R. W.; Echols, N.; Headd, J. J.; Moriarty, N. W.; Mustyakimov, M.; Terwilliger, T. C.; Urzhumtsev, A.; Zwart, P. H.; Adams, P. D. Towards automated crystallographic structure refinement with phenix.refine. *Acta Crystallogr., Sect. D: Biol. Crystallogr.* **2012**, *68*, 352−67.
(54) McPhillips, T. M.; McPhillips, S. E.; Chiu, H. J.; Cohen, A. E.; Deacon, A. M.; Ellis, P. J.; Garman, E.; Gonzalez, A.; Sauter, N. K.; Phizackerley, R. P.; Soltis, S. M.; Kuhn, P. Blu-Ice and the Distributed Control System: software for data acquisition and instrument control at macromolecular crystallography beamlines. *J. Synchrotron Radiat.* **2002**, *9*, 401−6.
(55) Winter, G. xia2: an expert system for macromolecular crystallography data reduction. *J. Appl. Crystallogr.* **2010**, *43*, 186−190.
(56) McCoy, A. J.; Grosse-Kunstleve, R. W.; Adams, P. D.; Winn, M. D.; Storoni, L. C.; Read, R. J. Phaser crystallographic software. *J. Appl. Crystallogr.* **2007**, *40*, 658−674.
(57) Moriarty, N. W.; Grosse-Kunstleve, R. W.; Adams, P. D. electronic Ligand Builder and Optimization Workbench (eLBOW): a tool for ligand coordinate and restraint generation. *Acta Crystallogr., Sect. D: Biol. Crystallogr.* **2009**, *65*, 1074−80.
(58) Chen, V. B.; Arendall, W. B., 3rd; Headd, J. J.; Keedy, D. A.; Immormino, R. M.; Kapral, G. J.; Murray, L. W.; Richardson, J. S.; Richardson, D. C. MolProbity: all-atom structure validation for macromolecular crystallography. *Acta Crystallogr., Sect. D: Biol. Crystallogr.* **2010**, *66*, 12−21.

DOI: 10.1021/acs.jmedchem.5b00609
J. Med. Chem. XXXX, XXX, XXX−XXX